

# bSlight: Battery-less Energy Autonomous Street Light Management System for Smart City

Prajnyajit Mohanty, *Graduate Student Member, IEEE*, Umesh C. Pati, *Senior Member, IEEE*, Kamalakanta Mahapatra, *Senior Member, IEEE* and Saraju P. Mohanty, *Senior Member, IEEE*

**Abstract**—Public lighting is a ubiquitous utility in cities to ensure the safety of people. In addition to playing a significant role in amending the comfort and safety of cities, street lighting causes substantial financial burden on governments to maintain its operation. Smart Light Emitting Diode (LED) street light system has become a prominent alternative to conventional street lighting systems with the involvement of Internet of Things (IoT). In this manuscript, a supercapacitor based smart street management system with energy autonomous capability has been proposed. It works in real-time and as an energy-saving alternative to prevent unnecessary electricity consumption of the street light. The average current consumption and power consumption of the system are 619.14  $\mu\text{A}$  and 2.022 mW, respectively. Three charging schemes have been investigated to find the optimized topology to harvest energy. The proposed device harvests energy from ambient sunlight and artificial light using a solar cell of 64 mm x 37 mm x 0.22 mm with maximum output power of 66 mW. LoRaWAN has been incorporated for communication, with a communication range of 761 m in real-world testbed. The operation characteristics and performance evaluation has been done based on implementing the system in field to ensure seamless operation.

**Index Terms**—Smart Cities, Smart Energy, Street Light Management, Energy Harvesting, Solar Energy, Supercapacitor, IoT, LoRaWAN

## 1 INTRODUCTION

TRENDS in global urbanization drive continuous advancements in digital technology and smart city design. It is anticipated that 68% of the global population will migrate from rural to urban areas by 2050 [1]. Therefore, smart city is a cynosure at the current time. The development of smart city applications has been significant in recent years. Intelligent street lighting is one of the most renowned among these applications. Cities now utilize 75% of the energy of the entire world, and street lights consume 30% to 40% of the total power of a city [2], [3]. Thus, energy efficiency is a considerable factor in designing any public lighting. Unceasing attempts have recently been made in this area by embracing Internet of Things (IoT). The framework of smart street light management system is shown in Fig. 1. However, the involvement of IoT in a wide range of applications causes a rapid surge in the number of IoT nodes around the globe. The number is likely to cross more than 30 billion by 2025 reportedly [4]. As a result, powering such a vast number of IoT nodes turns out to be a challenging problem that might impede the worldwide adoption of IoT.

Unfeigned efforts are being made to design batteryless energy autonomous IoT devices which can replace conventional battery powered ones. One such way to design batteryless energy autonomous IoT devices is to feed them



Fig. 1. Framework of smart street light management system

from various renewable energy resources such as solar, wind, thermal, mechanical vibration, radio frequency, etc. [5]. Although few energy autonomous IoT devices have recently been designed for several applications, most of them still rely on batteries for their energy requirements. The cost of wire, frequent replacement of batteries, and the impact of dead batteries on the environment has become the key concern for scientists. Despite the fact that there are not many alternatives to battery technology at the present time, supercapacitors are considered as a suitable substitute. Supercapacitors have been implemented as storage unit in wide range of applications such as automotive, consumer electronics, defense, and power industries due to their features like high power density, large number of charge cycles, fast charging, low cost, and long life.

- P. Mohanty, U. C. Pati, K. K. Mahapatra are with Department of Electronics and Communication Engineering, National Institute of Technology Rourkela, India.  
E-mail: prajnyajitmohanty@gmail.com, ucpati@nitrkl.ac.in, kkm@nitrkl.ac.in.
- Saraju P. Mohanty is with Department of Computer Science and Engineering, University of North Texas, Denton, TX.  
E-mail: saraju.mohanty@unt.edu

Manuscript is submitted on 22 Dec. 2023.

## 1.1 Contribution of the current paper

A smart street light management system has been proposed after reviewing the existing literature critically. The major contributions of the manuscript are as follows.

- The proposed system has been featured with energy autonomy. It is simultaneously powered from sunlight and artificial light.
- The system is made completely batteryless. Supercapacitor has been implemented as storage element.
- It adapts the illuminance level of the street light based on vehicle and pedestrian movements on the road. It can also identify and report the faulty street lights based on their light intensity to the concerned authorities through remote monitoring feature.
- It is incorporated with LoRaWAN for long range communication.
- It operates in real-time, demonstrating the feasibility of the system with energy harvesting.

## 1.2 Problems addressed in the current work and proposed solution

### 1.2.1 Implementation of supercapacitor over battery

The existing street light management systems are driven by conventional batteries, which have various drawbacks, including short lifespan, high cost, and the necessity for battery replacement [6]. Supercapacitor is widely adopted as an alternative to battery technology nowadays. Although supercapacitors feature fast charging, quick discharge is a crucial issue in supercapacitor based systems. In addition, it can store much less energy compared to battery due to its lower energy density characteristics. As a result, supercapacitor based systems can not provide long power back up as battery based systems. These factors make the implementation of supercapacitor challenging compared to batteries. Harvesting energy continuously and charging the supercapacitor uninterruptedly can be the solution to the cited issues. However, the availability of energy 24x7 in the outdoor environment is also a big concern. In this work, sunlight has been considered as the source of energy harvesting during day and street light has been considered as the source of energy harvesting during night. It has been accomplished using thinfilm solar cell and low power power management circuit.

### 1.2.2 Energy harvesting irrespective of time

Harnessing energy from sun light during the day has become easier with the advancement of photovoltaic technology. Most of the solar powered energy autonomous systems deployed in the outdoor environment use bigger size solar cells with output power in few watts and surface area of more than 100 cm<sup>2</sup> to maintain the required Quality of Service (QoS) [8], [9]. However, the cost and size of the device can be notable issues in that case. The aforementioned problem can be resolved using industry-grade monocrystalline solar cells with a modest surface area and relatively lower cost. On the other hand, energy harvesting during the night is extremely critical and a trending subject of research. Harvesting energy from sunlight during day and other renewable energy sources at night can be one

of the preferred solutions. However, adding multiple types of harvesters increases the complexity of the design. Few supercapacitor based PV powered energy autonomous IoT devices have been reported in recent past which can harvest energy during night at low light conditions. However, these devices are designed and tested for indoor uses during unavailability of sunlight. Design of a batteryless energy autonomous system for outdoor application which harvests energy during both day and night is crucial and challenging. In this work, a thinfilm based solar cell with cross section of 64 mm x 37 mm has been incorporated to harvest energy both from sunlight as well as artificial light during day and night continuously.

### 1.2.3 Power consumption of the device

The existing works are primarily concerned with expanding the features of the system, such as measuring different air quality factors, detecting gunshots, and integrating cameras with street light management system. However, the increased number of features implies increased power consumption. The power consumption of Wireless Sensor Network (WSN) and IoT devices has become one major issue that has not been addressed in most of the street light management systems. Therefore, the power consumption has been optimized using duty-cycle optimization technique. This technique has been implemented in some energy autonomous devices in the recent past; however, the percentage of duty cycle has been kept less in them to avoid power failure, implying lower QoS. The proposed device executes its primary objective continuously, i.e., controlling the illuminance of the street light in order to ensure high QoS. On the other hand, the remaining tasks are performed in duty cycle to minimize the overall power consumption of the device.

## 1.3 Novelty of the proposed work

The proposed work possesses the following novelty over the existing works.

- To the best of our knowledge, the proposed device is the first batteryless energy autonomous street light management system. It works in real-time and features self-sustainability complying green IoT paradigm.
- To the best of our knowledge, this is the first supercapacitor based street light management system. The device can harvest energy irrespective of time. The proposed system manages the operation of street light and harvests from the same during night when the availability of energy is critical. It signifies the ability of the device to manage energy effectively.
- The power consumption of the device has been optimized using the duty cycle optimization technique. As a result, it is found minimum compared to existing street light management devices.
- The percentage of duty cycle of operation is 50% which is more than triple compared to the state-of-the-art solar energy powered LoRaWAN based energy autonomous devices. Although the proposed device operates with such higher percentage of duty cycle, it is powered with relatively smaller size solar cell with cross sectional area

TABLE 1  
Comparison of State-of-the-art Smart Street Light Management Systems

References	Radio Technology	Sensing Parameters	Wireless Technology	Power Consumption	Energy Storage	Energy Autonomy	Power Optimization Technique
Kaleem <i>et al.</i> , 2016 [3]	ZigBee	Power, Light intensity, Motion	Short	384 mW*	N/A	No	No
Shahzad <i>et al.</i> , 2016 [10]	ZigBee	Light intensity, Temperature, Power	Short	414 mW*	N/A	No	No
Bellido-Outeirino <i>et al.</i> , 2016 [19]	ZigBee	Motion	Short	—	N/A	No	No
Daely <i>et al.</i> , 2017 [11]	ZigBee	Humidity, Power, Particle Concentration	Short	4.13 W*	N/A	No	No
Chen <i>et al.</i> , 2018 [18]	NB-IoT	Temperature, Humidity, Light intensity, and Power	Long	218 mW*	Battery	No	No
Abdullah <i>et al.</i> , 2018 [13]	N/A	Motion and Light intensity	N/A	387 mW*	Battery	No	No
Saha <i>et al.</i> , 2021 [12]	WiFi	Temperature, Humidity, Rain	Long	692.4 mW*	N/A	No	No
Sorif <i>et al.</i> , 2021 [14]	WiFi	Motion and Light intensity	Long	525 mW*	N/A	No	No
Sanchez-Sutil <i>et al.</i> , 2021 [15]	LoRaWAN	Motion, Current, Voltage	Long	—	N/A	No	No
Mohanty <i>et al.</i> , 2022 [49]	LoRaWAN	Motion, Light intensity	Long	2.012 mW	Battery	Yes	Duty cycle
<b>Current Paper (bSlight)</b>	LoRaWAN	Motion, Light intensity	Long	<b>2.022 mW</b>	<b>Supercapacitor</b>	<b>Yes</b>	<b>Duty cycle</b>

\*The power consumption of the work is not reported in the original manuscript. The value is calculated from the publicly available datasheets of the components for comparison purpose only. N/A represents the component is unavailable in this work. — represents that neither the direct data or its relevant data from which it can be calculated is available in the original manuscript.

of 2355.2  $mm^2$ . This is achieved due to the implementation of high efficient thinfilm type solar cell, ultralow power management circuit and energy-efficient low power off-the-shelf sensors and microcontroller.

- The proposed system is portable and can be fitted to any street light, such as solar-powered street lights, grid-powered street lights, and hybrid-powered street lights.

Furthermore, this paper is organized as follows: The related research work is discussed in Section 2. Section 3 discusses the proposed system architecture. Section 4 presents the design principles and considerations. The prototype and field testing details are explained in Section 5. Section 6 describes experimental validation, including operational characteristics and performance evaluation. The manuscript is concluded in Section 7.

## 2 RELATED RESEARCH WORK

There are many works reported regarding the design and development of smart street light management systems in the past. The comparison of the state-of-the-art street light management system has been shown in Table 1. In [10], intelligent street light system has been proposed to minimize the energy budget of a city by controlling the illuminance level of street light according to diurnal traffic volume. In [11] and [12], weather adaptive smart LED street light systems are designed to prevent road accidents. In [13] and [14], energy-saving methods have been proposed to conserve electricity in the smart city. In [15], a system has been designed to dynamically control the illumination levels by implementing Artificial Bee Colony (ABC) algorithm. In [17], the signature of received signal strength from the behaviors of vehicles as well as pedestrians moving on the roads is used to extract traffic parameters and the illuminance is controlled accordingly.

Street light management systems embedded with various communication technology have recently been proposed. In this direction, efforts have been made to feature long range and secure communication in street light system by implementing Narrow Band Internet of Things (NB-IoT) technology in [18]. In [19], a smart system based on wireless communication and Digital Addressable Lighting Interface (DALI) protocol has been designed to manage

public lighting. In [20] and [21], remote control-based intelligent LED street light systems are proposed incorporating ZigBee communication network. In [22], an energy-efficient lighting system incorporating ZigBee and General Packet Radio Service (GPRS) communication technology has been designed. In [24], a street light management system is designed implementing Artificial Intelligent (AI) technique. In [25], a Wireless Fidelity (WiFi) based smart system is proposed to control the illuminance level of the street light. In [26], a solar-powered street light management system is designed with commercially available off-the-shelf components. In [27], a secured street lighting management system comprises of web-based cloud management platform, edge devices, and real-time lighting control function. LoRaWAN based health monitoring solution has been proposed for soldiers deployed in hazardous environmental conditions in [28]. In [29], an energy-efficient smart metering system is proposed implementing Edge computing in Long Range (LoRa). Further, LoRaWAN has been implemented for different solar energy powered IoT devices in [30], [31], [32]. In these works, LoRaWAN based systems are tested in real-time. Energy-efficient algorithms have been proposed for minimizing the power consumption of LoRa in water quality systems in [34] and [35]. In [36], solar energy powered LoRa based air quality monitoring device has been designed for environmental parameter measurement. However, optimization in size of the solar cell size, energy storage unit, and energy requirement of the application is essential for solar energy powered systems which is addressed in [37].

Design of batteryless systems is a major topic of interest in current scenario. In [38], a solar powered batteryless environment parameter monitoring device is proposed which features long range communication through LoRaWAN. In [40], a batteryless indoor air quality monitoring device is designed which can harvest energy in indoor light condition. In [41], a batteryless bluetooth beacon has been designed and tested for pushing advertisements on screen. Supercapacitors have been used as energy storage component in these batteryless systems.

## 3 PROPOSED SYSTEM ARCHITECTURE

The proposed system is an energy autonomous street light management system. Fig. 2 illustrates the block diagram of

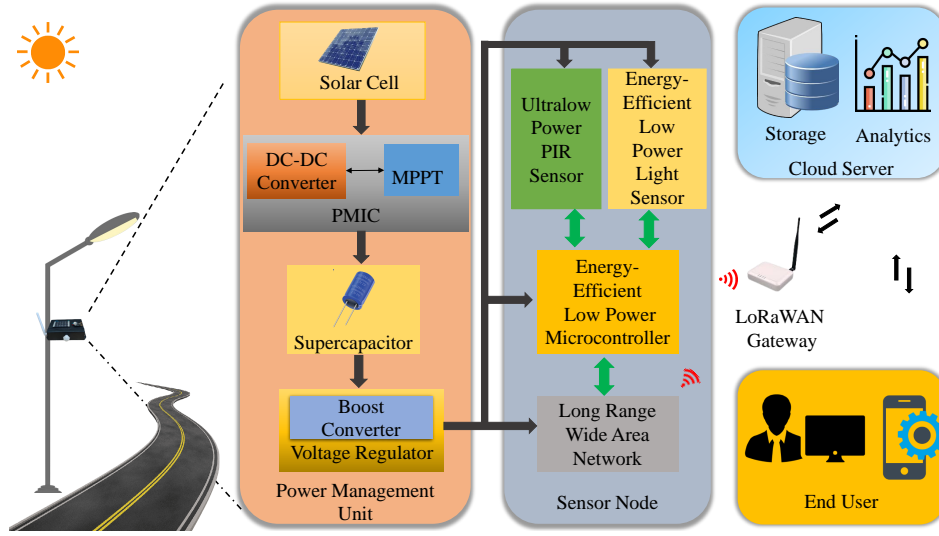


Fig. 2. Block diagram of the proposed system

proposed system. The design of the system is broken down as follows:

### 3.1 Power Management Unit

This unit is responsible for harnessing, optimizing, storing and regulating the energy as per the requirement of the sensor node. It includes solar cells that can harvest energy from sunlight and artificial light. A Power Management Integrated Circuit (PMIC) manages the harvested power. It consists of two cascaded DC-DC switching converters, namely the boost converter and the buck converter with high-power conversion efficiency. It steps up or steps down the output voltage of the solar cell to a maximum of 3 V and output current of 110 mA. It also features Maximum Power Point Tracker (MPPT), which optimizes the harvested power and provides it to the supercapacitor. It wakes up every 5 seconds to perform the MPPT calculation to ensure that the supercapacitor is provided with optimized amount of power from solar energy. The internal logic of the PMIC guarantees tight monitoring of both the overcharge ( $V_{OVCH}$ ) and minimum acceptable voltage by the supercapacitor ( $V_{OVDIS}$ ). A single-cell supercapacitor has been used for storing energy. The sensor node should be necessarily operated at a recommended voltage in order to perform effectively. A high efficient with ultralow quiescent current ( $I_q$ ) buck-boost regulator has been used to convert the output of the supercapacitor to 3.3 V.

### 3.2 Sensor Node

It performs sensing, processing, and communication of the data. It contains a microcontroller, sensors, and a LoRa module. All the components in the sensor node are low-power variants. It measures two parameters: movement/occupancy using a Passive Infrared (PIR) sensor and light intensity with the help of a light sensor. The microcontroller supports ARM cortex M0 based architecture. It processes the PIR sensor signal and generates a Pulse Width Modulation (PWM) control signal, which is later sent to the AC dimmer module. The dimmer module controls the

current to the street light in order to make it illuminate at 100% or 50% illuminance. LoRaWAN technology has been incorporated for data communication. The microcontroller sends the working status of the street light to the LoRaWAN gateway. It possesses high sensitivity of -148 dBm and features long range communication.

### 3.3 LoRaWAN Gateway

It serves as a conduit between the cloud server and the sensor node. It exchanges information with the cloud server after receiving data from the sensor node through MQTT broker. Symmetric encryption is used to encrypt the data sent through LoRa. MQTT protocol has become increasingly popular in IoT due to characteristics like low power consumption, quick data transfer, lightweight design, and simplicity of implementation.

### 3.4 Cloud Server and End User

Cloud storage is used to store the data received from the LoRaWAN gateway. It consists of two subunits such as cloud storage and analytics. The cloud storage unit stores the data received from the sensor node, whereas the cloud analytics unit provides valuable insights to the end user. The end user can monitor the data coming from the sensor node in real-time. It provides a visually appealing Graphical User Interface (GUI) for use in remote monitoring. A mobile application and web portal are available to the end user for data access.

Further, the flowchart of the power-aware software algorithm of bSlight has been shown in Fig. 3. It has been programmed to perform efficiently and consumes less energy. The duty cycle optimization technique is implemented for its operation. It harvests energy during day with average current ( $I_{charge}$ ) of 7.91 mA and the voltage level of supercapacitor ( $V_{supercap}$ ) increases gradually. The voltage regulator results 3.3 V to the system once  $V_{supercap}$  crosses 1.8 V. Thus, the system starts its function by measuring light intensity to decide whether it is day or night. It turns off the street light during day. The device extracts energy from the

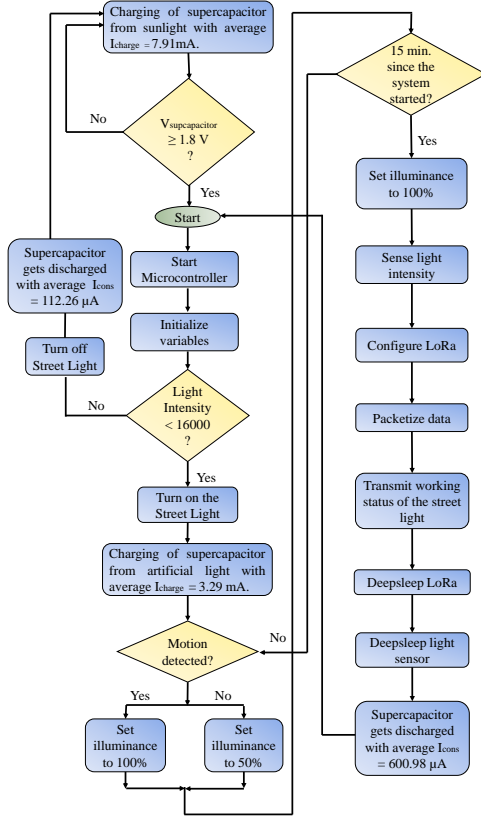


Fig. 3. Power-aware software algorithm of bSlight

supercapacitor with an average current consumption ( $I_{cons}$ ) of  $112.26 \mu\text{A}$  from the supercapacitor during day. It starts its full phase operation once the light intensity drops below  $16000 \text{ lux}$ . It turns on the street light in the first step. In this phase, the device harvests energy from the street light and the supercapacitor gets charged with an average current of  $3.29 \text{ mA}$ . Further, it continuously detects pedestrian or vehicular motion around the road. It sets the illuminance of the street light at  $100\%$  if any motion is detected. The illuminance is reduced to  $50\%$  otherwise. Hereafter, it can monitor the working status of the street light by sensing its light intensity. It is generally observed that street lights do not glow with their specified light intensity often, which can catalyze road accidents. Hence, bSlight measures the light intensity at  $100\%$  illuminance level and verifies whether the street light is faulty. Subsequently, it sends the working status to the LoRa gateway. Then it puts LoRa and the light sensor into a deep sleep mode for approximately 15 minutes. The supercapacitor gets discharged with  $I_{cons}$  of  $600.98 \mu\text{A}$  during night. It can be noted that  $I_{cons}$  is relatively higher than that of during day as the system performs its major functions during night. The admin can easily visualize the working status of each street light around the city through a local GUI and find the faulty one. It turns off the street light once it detects sunlight and repeats the process.

#### 4 DESIGN PRINCIPLES AND CONSIDERATIONS

Energy harvesting enabled IoT nodes should meet self-sustainability criteria in order to operate perpetually. Ap-

plication requirements and hardwares should be critically considered in order to satisfy the above criteria. The system is typically intended for outdoor uses.

#### 4.1 Energy Harvesting

Solar energy possesses higher power density and output voltage compared to other energy sources [7]. It is a preferred energy source in outdoor applications due to its ubiquity. The output power of a solar cell ( $P_{solar}$ ) can be expressed using (1).

$$P_{solar} = V_{solar} \times I_{solar} \quad (1)$$

where  $V_{solar}$  and  $I_{solar}$  are output voltage and output current of the solar cell. There have been several developments in solar energy harvesting technology in recent days. Various types of solar cells are commercially available such as polycrystalline, monocrystalline, thinfilm, perovskite, etc. Monocrystalline type solar cell provides improved efficiency for harvesting solar energy during the presence of sunlight, and thinfilm type solar cells are promising technology for harvesting energy from intermediate and artificial light. The application demands energy harvesting during both the day and night. Therefore, monocrystalline and thinfilm type solar cells can work as suitable options for energy harvesting due to their specific features, efficiency, and cost-effectiveness. In this work, attempts have been made to harvest energy using three different schemes. The schemes are as follows.

- Scheme 1: Energy harvesting using a monocrystalline solar cell denoted as  $PV_1$ , which performs best under direct sunlight.
- Scheme 2: Energy harvesting using series connection of a  $PV_1$  and a thinfilm solar cell denoted as  $PV_2$ , which is specifically designed for indoor as well as low light conditions i.e.  $200 \text{ lux}$ .
- Scheme 3: Energy harvesting using a thinfilm solar cell named as  $PV_3$ , designed for harvesting energy in intermediate light conditions.

#### 4.2 Energy Storage

There are mainly two options for storing harvested energy in IoT nodes which are battery and supercapacitor. Batteries possess more energy density and less power density which makes them suitable option to be used in IoT devices. However, batteries are not eco-friendly options. Supercapacitors are adopted widely as an alternative energy storage element in IoT devices due to their long life and fast charging feature compared to batteries. The energy stored in the supercapacitor can be expressed using (2).

$$E_{supercap} = 0.5 \times C \times V_{supercap}^2 = \epsilon_D W \quad (2)$$

where  $E_{supercap}$  is the amount of energy stored in the supercapacitor.  $\epsilon_D$  and  $W$  are the energy storage density and weight of the supercapacitor. In this work, the value of  $\epsilon_D$  is  $1.32 \text{ Wh/kg}$  defined by the manufacturer. The ideal and conventional way of solar energy harvesting is to enable energy harvesting during day and storing it in a energy storage unit for use in night. However, this is not applicable to aforementioned application due to less value of  $\epsilon_D$  of

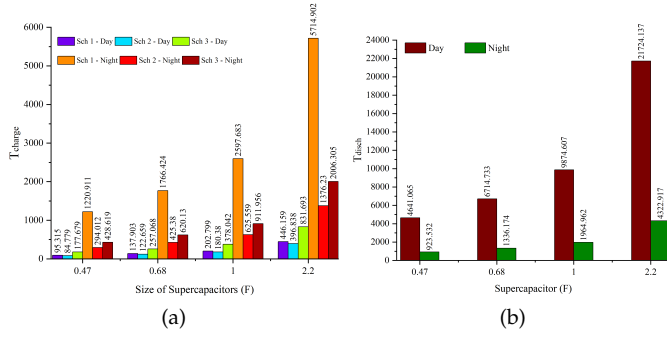


Fig. 4. Simulation results (a) charging time of supercapacitors during day and night (b) discharging time of the supercapacitors during day and night

the supercapacitor. Supercapacitor can be incorporated in case the energy harvesting is always greater than or equal to energy consumption irrespective of time. This can be represented mathematically using (3).

$$\int_{T_1}^{T_2} P_{solar} dt \geq \int_{T_1}^{T_2} P_{cons} dt \quad (3)$$

where  $P_{cons}$  is the average power consumption of the sensor node along with voltage regulator. Further, the size of supercapacitor should be carefully selected so that power failure of the device will not be encountered at any point of time. An existing mathematical model in [39] is simulated in order to find the optimized size of the supercapacitor needed to drive the system. The model results charging time ( $T_{charge}$ ) and discharging time ( $T_{disch}$ ) of supercapacitor considering practical parameters such as leakage current ( $I_{leakage}$ ) and equivalent series resistance ( $R_{esr}$ ). Let's presume that the supercapacitor is in a zero-charge condition before the charging process begins, which implies that the voltage across the capacitor is zero. When  $t \geq 0$ , the charging voltage of the supercapacitor can be expressed by (4).

$$C_{sc} \frac{dV_{sc}}{dt} + \frac{V_{sc}}{R_{dcl}} - I_{charge} = 0 \quad (4)$$

where  $C_{sc}$  and  $V_{sc}$  are the capacitance and voltage across the supercapacitor, respectively.  $R_{dcl}$  and  $I_{charge}$  represent the leakage resistance and charging current of the supercapacitor, respectively. The average  $I_{charge}$  has been calculated from the measured values.  $I_{charge}$  is calculated as 14.69 mA and 1.16 mA for scheme 1 during day and night, respectively. The same is computed in the case of scheme 2

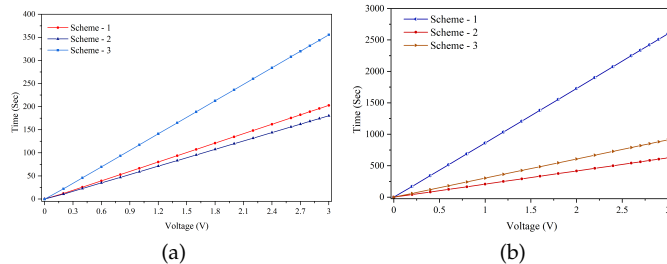


Fig. 5. Simulated charging curve of 1 F supercapacitor when the system is disconnected under (a) natural sunlight (b) artificial light

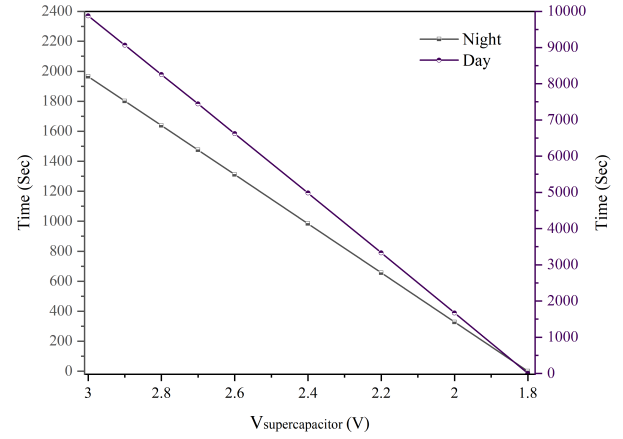


Fig. 6. Simulated discharge curve of 1 F supercapacitor during operation of the device while the charging is stopped

as 16.5 mA and 4.79 mA during day and night, respectively. It is calculated as 7.91 mA and 3.29 mA for day and night, respectively, in case of scheme 3. Further, the final output voltage of the supercapacitor ( $V_{out}$ ) can be derived using (5).

$$V_{out} = I_{charge} R_{esr} + I_{out} R_{dcl} \left( 1 - \exp \left( -\frac{T_{charge}}{R_{dcl} C_{sc}} \right) \right) \quad (5)$$

$R_{esr}$  is obtained from manufacturer datasheet as  $1.5 \Omega$ .  $R_{dcl}$  has been measured as  $259147.451 \Omega$ . The charging curve of the supercapacitor during day and night is shown in Fig. 4. The discharge process with constant current  $I_{cons}$  due to the operation of the device can be started once  $V_{out}$  reaches its maximum value, which is denoted as  $V_{sc}^0$ . In this work,  $V_{sc}^0$  can be considered as 3 V. This condition is expressed mathematically in (6).

$$\frac{1}{C_{sc}} \int_{t=0}^{t=T_{disch}} I_{sc} dt + I_{sc} R_{dcl} - (V_{sc}^0 + I_{cons} R_{dcl}) = 0 \quad (6)$$

where  $I_{sc}$  represents the current across supercapacitor. Finally,  $V_{out}$  can be expressed after the system is operated for  $T_{disch}$  seconds using (7).  $V_{out}$  is supposed to be 1.79 V due to the operation of the system after which the supercapacitor will not be able to run the system.

$$V_{out} = -I_{out} R_{esr} + V_{sc}^0 - \left( (V_{sc}^0 + I_{out} R_{dcl}) \left[ 1 - \exp \left( -\frac{T_{disch}}{R_{dcl} C_{sc}} \right) \right] \right) \quad (7)$$

In order to calculate  $T_{disch}$  from this model, the current consumption data of the device is required. The current consumption measurement and calculations has been shown in experimental validation section. The average  $I_{cons}$  has been calculated from measurement data. The major functions of the device is done during night and the average  $I_{cons}$  is calculated as  $600.98 \mu A$  during this period. The same during daytime is calculated as  $112.26 \mu A$ . Fig. 4 shows  $T_{charge}$  and  $T_{disch}$  of supercapacitors of four different values. As a design consideration, it is considered that the device should be able to run a minimum of one cycle, i.e. 900 seconds when the supercapacitor is fully charged. As a result, the device can get sufficient time to charge the

supercapacitor in harsh weather conditions. This can ensure that the device can safely overcome the slow charging phase under poor lighting conditions such as heavy rain and foggy weather. Since the device can only perform when the output voltage of the supercapacitor lies in the range of 3 V to 1.8 V, this criteria can be written mathematically using (8) where  $T_2 \geq 900$ .

$$E_{supercap} \geq 1.5625 \times \int_{T_1}^{T_2} P_{cons} T_{disch} dt \quad (8)$$

Thus, a supercapacitor of size 0.47 F and above satisfy this criteria. However,  $T_{charge}$  also increases with the size of the supercapacitor, which should be necessarily as low as possible to ensure fast charging. Thereby, based upon the simulation results, 0.47 F supercapacitor can be considered as the optimized supercapacitor size for the device. Nevertheless,  $T_{disch}$  can also be calculated from mathematical expression as presented in (9).

$$T_{disch} = 0.64 \times \frac{E_{supercap}}{P_{cons}} \quad (9)$$

$P_{cons}$  has been measured as 1.98 mW. Thus,  $T_{disch}$  is calculated as 683.63 seconds, 989.09 seconds and 1454.54 seconds for 0.47 F, 0.68 F and 1 F supercapacitor, respectively. Experiments are conducted to verify  $T_{disch}$  of these supercapacitors.  $T_{disch}$  is measured as 654 seconds, 791 seconds, and 1103 seconds for 0.47 F, 0.68 F, and 1 F supercapacitor, respectively. Therefore, the optimized size of the supercapacitor is considered as 1 F in this work. The charging curve and discharging curve of supercapacitor of 1 F according to the mathematical model is shown in Fig. 5 and Fig. 6, respectively. The peak current that can be drawn from the supercapacitor is 0.81 A as per the manufacturer datasheet which is much greater than the requirement of this work. The power density of the same is 1322 W/kg which satisfies the requirement of the proposed device easily.

## 5 PROTOTYPE AND FIELD TEST

As the initial step of the prototyping, a high efficient off-the-shelf PMIC with power consumption below 1 mW should be incorporated in order to satisfy ultra-low power consumption range [23]. The PMIC used in this work, is configured according to the supercapacitor input requirements and demand of the application. Although an off-the-shelf PMIC has been incorporated for energy harvesting, some external resistor values must be calculated and used following the design rules and equations by the manufacturer of the PMIC

TABLE 2  
Component details of the bSlight

Component	Part
Solar cell	SP3-37, LL200-3-37, SM141K06L
PMIC	AEM10941
Supercapacitor	SCCR12E105PRB
PIR sensor	EKMB1103111
MCU	STM32L010C6
Light sensor	VEML7700
Wireless module	RFM95
Buck-Boost Regulator	MAX77827

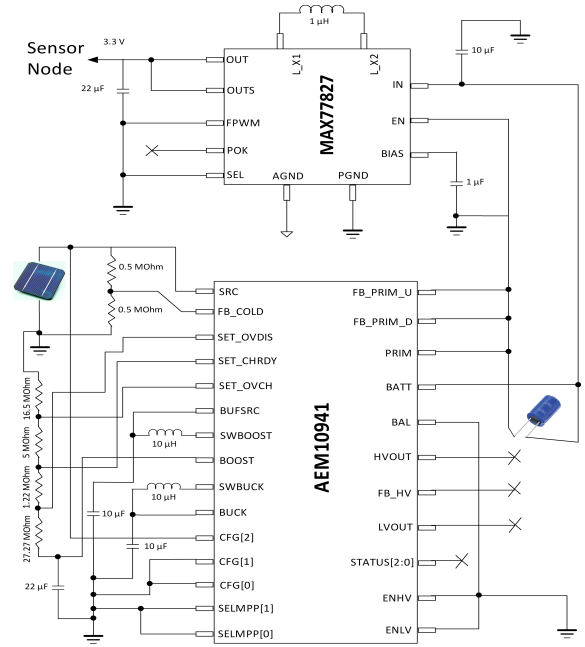


Fig. 7. Power management circuit of bSlight

in order to ensure effective power management [42]. The solar cell produces voltage ranging from 0 V – 4.6 V, and the supercapacitor can be charged with a maximum voltage of 3 V. Thus, the PMIC has been configured in buck-boost mode in this work. The storage unit is a single cell supercapacitor; thus, CFG [2:0] has been configured, as shown in Fig. 7. The maximum acceptable voltage of the supercapacitor is 3 V which can be set through the  $V_{OVCH}$  of the PMIC. When the voltage of the supercapacitor reaches  $V_{OVCH}$ , the charge is completed, and the internal logic keeps the output voltage of the PMIC ( $V_{BATT}$ ) at or near  $V_{OVCH}$  with a hysteresis of a few millivolts to protect the storage element and the electronics.  $V_{OVDIS}$  is set at 2.2 V as this voltage can range from 2.2 V – 4.4 V. The PMIC features two LDO; however, they are not used in this work which is the reason for grounding the pins ENHV and ENLV. Although any of the LDO of the PMIC has not been used in this work, ‘SET\_CHRDY’ can not be left floating. Thus, it is set at 2.325 V as it can be set between any value ranging from 2.25 V – 4.45 V. The responsible external resistors are

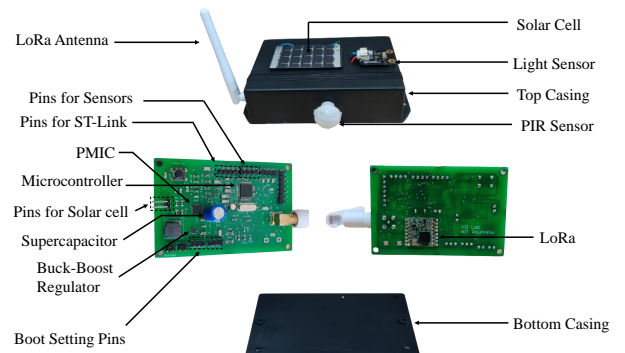


Fig. 8. The designed prototype of bSlight

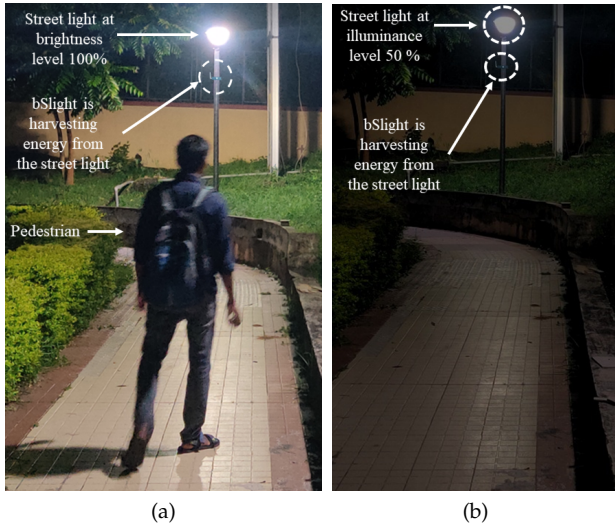


Fig. 9. Implementation of the bSlight with a street light in garden area (a) illuminance is set at 100% upon detection of movement (b) illuminance is 50% on empty road condition

calculated as  $16.5 \text{ M}\Omega$ ,  $5 \text{ M}\Omega$ ,  $1.22 \text{ M}\Omega$ , and  $27.27 \text{ M}\Omega$ . The PMIC also features a cold start unit. The minimum required input voltage is  $380 \text{ mV}$ , and the minimum input power is  $3 \mu\text{W}$  for it to begin functioning with empty storage components. In this work, the cold start voltage is set as  $0.76 \text{ V}$  as the solar cell is intended to get enough light to produce sufficient voltage irrespective of time. The resistors responsible for setting the cold start voltage are calculated as  $0.5 \text{ M}\Omega$  both. The PMIC can extract the power from the source as long as the input voltage lies between  $50 \text{ mV}$  and  $5 \text{ V}$  after the cold start. The PMIC features MPPT for optimizing the harvested power. The MPP ratio of the solar cell is calculated as the ratio of maximum power point voltage ( $V_{MPP}$ ) and open circuit voltage ( $V_{OC}$ ) which is around 65% to 73%. Thus, the Maximum Power Point (MPP) of the PMIC is set as 70% by grounding the SELMPP [1] and SELMPP [0] pins as described in the design rule [42]. The capacitor values are taken as per the datasheet of the PMIC. The component details of bSlight have been presented in Table 2. It has been designed with a satisfactory form factor, i.e.,  $125\text{mm} \times 85 \text{ mm} \times 25\text{mm}$ , so that it can fit with any

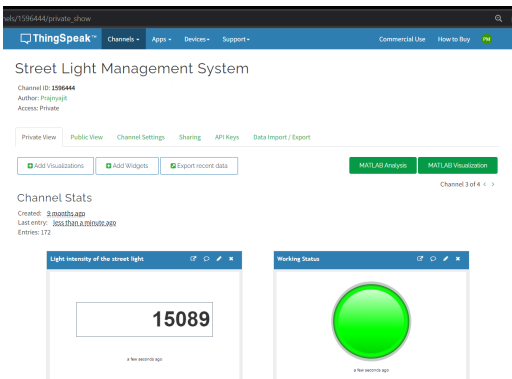


Fig. 10. Light intensity and working status of the street light is shown through the GUI

street light poles. The circuit is printed on FR4 based Printed Circuit Board (PCB). The details of the designed prototype are shown in Fig. 8. The proposed bSlight is installed with a street light in the garden area of a hostel to examine its feasibility. Fig. 9 shows the implementation of bSlight with a street light. The data from bSlight gets uploaded to the ThingSpeak cloud storage through the LoRa gateway. The cloud service features GUI through which the authority can monitor the operational status of individual street lights. Fig. 10 represents the light intensity and working status of the street light reflecting on ThingSpeak GUI. Further, the experimental results in various conditions have been shown in experimental validation section.

## 6 EXPERIMENTAL VALIDATION

### 6.1 Characteristics of Solar Cell

The PV and IV characteristics are observed for all three solar cells and are shown in Fig. 11. The characteristics have been observed under two different conditions such as under direct sunlight and under artificial light. The intensity of the arti-

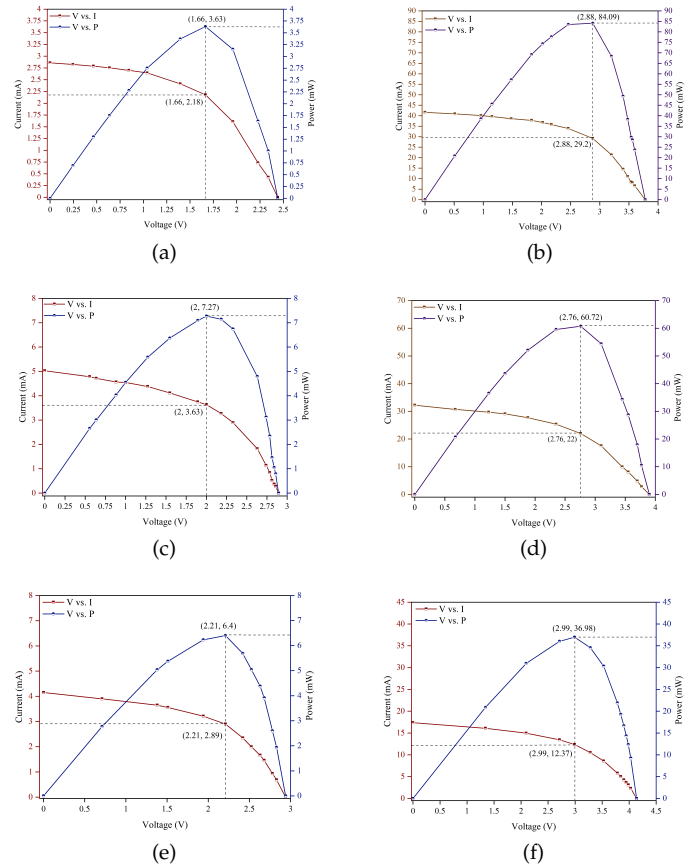


Fig. 11. VI characteristics of solar cells (a)  $PV_1$  under artificial light (b)  $PV_1$  under direct sunlight (c)  $PV_2$  under artificial light (d)  $PV_2$  under direct sunlight (e)  $PV_3$  under artificial light (f)  $PV_3$  under direct sunlight

ficial light is kept at 15000 lux, which is the intensity under the street light where bSlight is installed. The intensity of light has been measured using HTC LX-101A. The MPP ratio of  $PV_1$  under direct sunlight and artificial light is observed approximately 76% and 66%, respectively. The same for  $PV_2$  is 70% and 69% in the presence of sunlight and artificial



light, respectively. The MPP ratio of  $PV_3$  is 72% and 75% in the presence of sunlight and artificial light, respectively.

## 6.2 Performance of PMIC

PMIC optimizes the output power of the solar cell. There are two major roles of PMIC in this work. Firstly, it delivers a maximum of 3 V to the supercapacitor so that it can be charged. Secondly, it tracks MPP to ensure that the system can harvest maximum power every time. These two features of PMIC can be observed in Fig. 12, taken during its operation under experimental conditions. The output voltage of solar cell is fluctuating and varies in the range of 2.83 V – 4.04 V due to factors like cloud movement, wind, humidity, temperature, etc. MPPT status is asserted as shown in Fig. 12, evidencing that MPP operation is performed. MPPT feature in the PMIC enables it to wake up every 5 seconds to perform MPP operation. The supercapacitor is charged up to 3 V under this circumstance. The output voltage of the supercapacitor reaches 3 V approximately in 397 seconds, after which MPP operation gets slower, and the duration of MPP calculation increases.

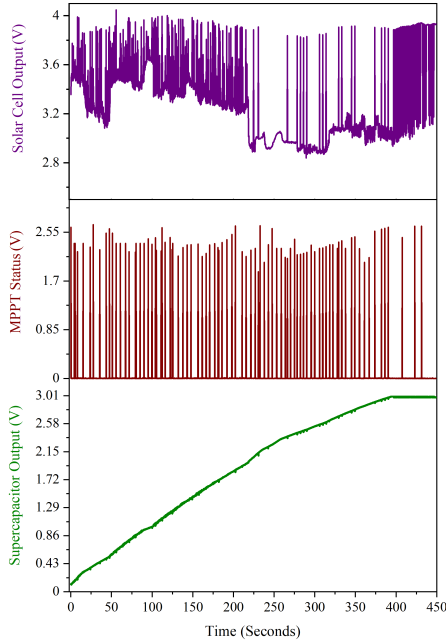


Fig. 12. Operation of PMIC in the presence of sunlight

## 6.3 Powering the Sensor Node

The supply voltage requirement of components in the sensor node varies from 2.3 V - 3.6 V. Thus a constant input voltage must be supplied to the sensor node. Fig. 13 shows the output voltage of the supercapacitor and that of the buck-boost regulator, which is used to provide a constant voltage of 3.3 V to the sensor node. The supercapacitor is discharged with a constant current, and simultaneous output voltage from the regulator is recorded. This ensures that the supercapacitor can drive the device until its output voltage level lies below 1.8 V. The device can not be powered if the output voltage of the supercapacitor further lies below 1.8 V. Further fall in the output voltage of the supercapacitor

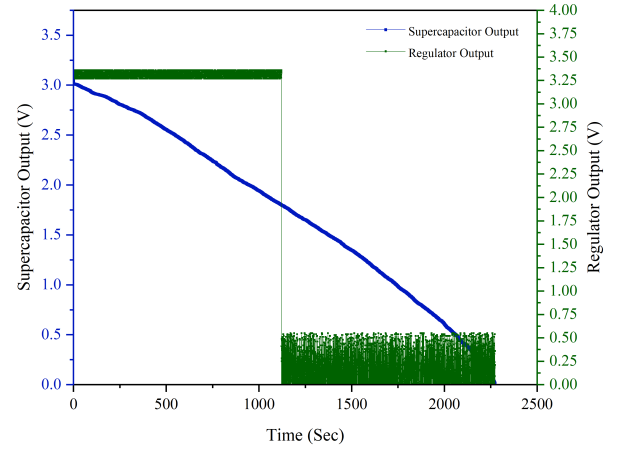


Fig. 13. Output voltage of buck-boost regulator and output voltage of the supercapacitor

leads to a sharp fall in the output voltage of the regulator, which is much below the voltage requirement of the sensor node.

## 6.4 Current Consumption of the Device

The current consumption of the device is shown in Fig. 14. It varies during day and night. The major functions of bS-light are performed during night when all the components of the sensor node come into active mode. The average measured current consumption of the components in the sensor node and PMU has been reported in Table 3. PIR sensor and microcontroller never go into deep sleep mode during night due to continuous operation, while LoRaWAN and light sensor wake up periodically to perform necessary operations. The total average current consumption of the device ( $I_{sys}$ ) during night has been calculated using (10).

$$I_{sys} = \frac{1}{T_{Total}} (I_{APIR} \times T_{APIR} + I_{DPIR} \times T_{DPIR} + I_{AMCU} \times T_{AMCU} + I_{DMCU} \times T_{DMCU} + I_{ALS} \times T_{ALS} + I_{DLS} \times T_{DLS} + I_{ALoRa} \times T_{ALoRa} + I_{DLoRa} \times T_{DLoRa} + I_{Reg} \times T_{Reg} + I_{PMIC} \times T_{PMIC}) \quad (10)$$

$I_{APIR}$ ,  $I_{AMCU}$ ,  $I_{ALS}$ , and  $I_{ALoRa}$  represent the average current consumption of the PIR sensor, microcontroller, light

TABLE 3  
Summary of Measured Current Consumption

Component	Current	Duration (Sec)		Mode
		Day	Night	
PIR Sensor	124 $\mu$ A	0	900	Active
	3.17 $\mu$ A	900	0	Deep Sleep
Microcontroller	431 $\mu$ A	1	900	Active
	81 $\mu$ A	899	0	Deep Sleep
Light Sensor	62 $\mu$ A	0.1		Active
	1.5 $\mu$ A	899.9		Deep Sleep
LoRa	71.67 mA	0	0.23	Active
	8.5 $\mu$ A	900	899.77	Deep Sleep
Regulator	17.66 $\mu$ A	900		Active
PMIC	18.16 $\mu$ A	900		Active

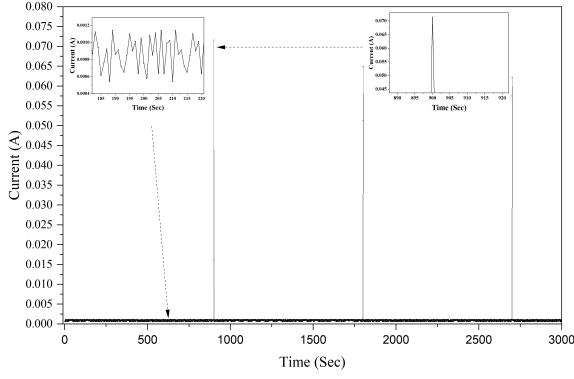


Fig. 14. Current consumption of the bSlight during night

sensor, and LoRa module in the active mode, respectively.  $I_{DPIR}$ ,  $I_{DMCU}$ ,  $I_{DLS}$  and  $I_{DLoRa}$  are the average current consumption of the PIR sensor, microcontroller, light sensor, and LoRa module in deep sleep mode, respectively.  $T_{APIR}$ ,  $T_{AMCU}$ ,  $T_{ALS}$ , and  $T_{ALoRa}$  represent the working duration of the PIR sensor, microcontroller, light sensor, and LoRa module in the active mode, respectively.  $T_{DMCU}$ ,  $T_{DPIR}$ ,  $T_{DLS}$ , and  $T_{DLoRa}$  are considered as the time duration of microcontroller, PIR sensor, light sensor and LoRa module in deep sleep mode, respectively.  $I_{Reg}$ ,  $I_{PMIC}$  and  $T_{Reg}$ ,  $T_{PMIC}$  represent the current consumption and time duration of the operation of the buck-boost regulator and PMIC, respectively. The duration of one cycle is denoted by  $T_{Total}$  which is considered 900 seconds since the device is programmed to repeat the operation every 15 minutes.  $I_{sys}$  has been calculated as  $619.14 \mu A$  during night which is the maximum average current consumption at anytime. As per the system architecture of bSlight, supercapacitor is used to power the sensor node along with the buck-boost voltage regulator. However, PMIC works consuming power from solar cell. The average current consumption of the sensor node along with voltage regulator during night can be calculated as  $600.98 \mu A$  which is termed as  $I_{cons}$ . The same can be calculated during day as  $112.26 \mu A$ . The maximum power consumption of the bSlight ( $P_{sys}$ ) is measured as 2.022 mW.

### 6.5 Supercapacitor charging and operational characteristics

In order to observe the charging characteristics of the supercapacitor, it is charged under the sunlight during day and artificial light i.e. 15000 lux during night when the load is disconnected. The supercapacitor can drive the system unless its output voltage lies below 1.8 V. This signifies that although the supercapacitor has a capacitance of 1 F, the system can only utilize 64% of its energy. The charging curves of the supercapacitor using all three schemes are shown in Fig. 15. The total charging time of the supercapacitor in practical scenario is 222.33 seconds and 2863.32 seconds to get charged from 0.2 V to 3 V and 0.28 V to 3 V, respectively, using scheme 1 under sunlight and artificial light, respectively. The same has been measured as 95.31 seconds and 1671.54 seconds during day and night using the same scheme to get charged from 1.8 V to 3 V, respectively. The

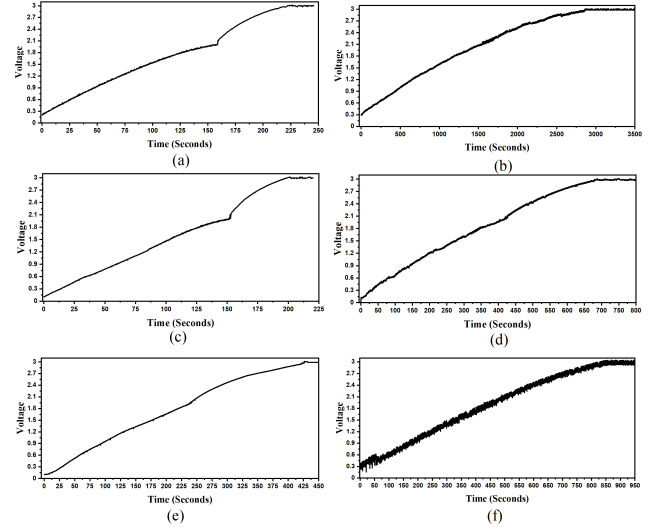


Fig. 15. Charging of supercapacitors using different schemes when the load is disconnected (a) Scheme 1 during day (b) Scheme 1 during night (c) Scheme 2 during day (d) Scheme 2 during night (e) Scheme 3 during day (f) Scheme 3 during night

supercapacitor takes 199.5 seconds to get charged from 0.1 V to 3 V when exposed to sunlight using scheme 2, whereas it takes 687.28 seconds to get charged from 0 V to 3 V when exposed to artificial light using the same scheme. Thus, it takes 71.75 seconds and 341.77 seconds using scheme 2 to get charged from 1.8 V to 3 V under sunlight and artificial light, respectively. The supercapacitor takes 426.13 seconds to get charged from 0.1 V to 3 V under sunlight using scheme 3. Subsequently, the same takes 816.18 seconds to get charged from 0.32 V to 3 V under artificial light using scheme 3. The charging time has been observed as 206.09 seconds and 385.06 seconds during day and night to get charged from 1.8 V to 3 V, respectively, using scheme 3. However, indoor solar cell which is specifically designed for working under room light conditions, does not work well when exposed to direct sunlight due to high chances of material degradation. The performance of this solar cell can be reduced to 50% if it is exposed to sunlight for 100 hours, according to the manufacturers of the solar cell. This restricts the implementation of scheme 2 for powering the device. The device stays in low power mode in the day and performs its primary operations during night. The charging time of the supercapacitor is very high during night in case of scheme 1, unlike scheme 3, which is a major disadvantage of scheme 1. The energy harvested using scheme 3 under sunlight is very high compared to the consumed energy during the day. This ensures that scheme 3 can be the optimized method for charging the device.

It is indeed challenging to implement supercapacitors for outdoor applications where energy expenditure during night is excessive, and energy availability is critical. The charging rate should always be greater compared to discharging rate when the device is running in order to avoid any futile circumstances. Further, the charging time of the supercapacitor from 1.8 V to 3 V at various luminosity has been plotted in Fig. 16. The illuminance level of street light lies in the range from 7412 lux to 7543 lux when there is no

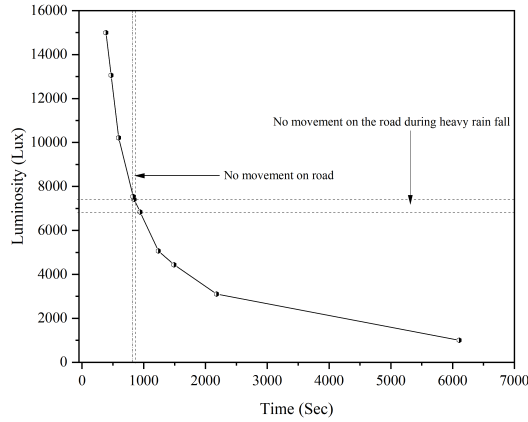


Fig. 16. Charging time of 1 F supercapacitor at various luminosity

movement on the road. The corresponding charging time of the supercapacitor ranges from 827 seconds to 843 seconds. Charging time increases under low light condition. Thereby, it is measured under raining condition considering it as a worst-case scenario. The measured charging time goes up to 941 seconds under heavy rain and empty road conditions. The discharge time of the supercapacitor is measured as 1103 seconds when bSlight is performing the tasks which it executes during night and the solar cell is completely disconnected. The device should necessarily comply (11) in order to ensure the seamless operation.

$$T_{charge} \leq T_{disch} \quad (11)$$

Fig. 17 presents the output voltage of the supercapacitor in four different phases. In the first phase, the supercapacitor is fully charged when it is neither connected to the solar cell nor the load. Thus, the output voltage is constant at around 3 V, and the corresponding solar cell voltage is 0 V. In the second phase, the supercapacitor voltage is reduced to 1.8 V. The supercapacitor is connected and the device executes all the tasks it should execute during the night. In this phase, the solar cell is disconnected, which is why the corresponding output voltage of the solar cell is at 0 V. This phase signifies the discharge time of the supercapacitor, which is measured as 1103 seconds. In the third phase, the

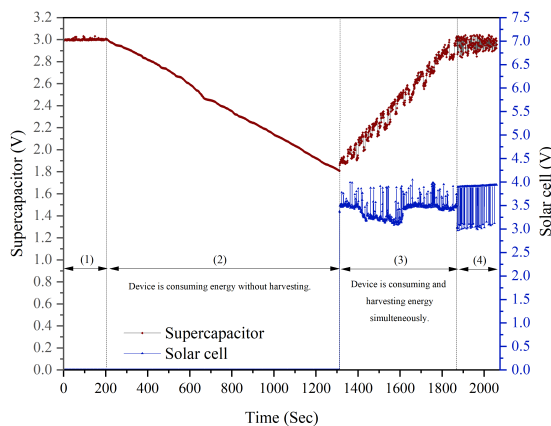


Fig. 17. Output voltage of the supercapacitor and solar cell during different operational conditions

bSlight harvests and consumes energy simultaneously. It performs all the operations that must be done during night. In the last phase, the supercapacitor is fully charged while both harvesting and consumption of energy are ongoing. Further, self-discharge process of the supercapacitor is one of the major issues which can cause power failure in any supercapacitor based device. Although bSlight can harvest energy during heavy rain, the illuminance level critically goes as low as 6835 lux during this condition.  $I_{leakage}$  of the supercapacitor has been measured in practical scenario during typical rainy weather in order to ensure that the device can sustain power failure condition due to the self-discharge issue of the supercapacitor. Fig. 18 presents the self-discharge process of the supercapacitor. The supercapacitor is remained in open circuit for approximately 72 hours. The temperature during the experiment varies between 30 °C – 34.5 °C in day and 26 °C – 30 °C in night. Subsequently, Relative Humidity (RH) varies in the range of 50 % – 70 % during day and 75 % – 95 % during night. The leakage current can be calculated using the below equation.

$$I_{leakage} = \frac{C \times \Delta V}{\Delta T} \quad (12)$$

where C represents the capacitance of the supercapacitor, which is 1 F in this work.  $\Delta V$  is the change in the voltage level of the supercapacitor due to self-discharge, which is 3 V for this experiment.  $\Delta T$  presents the total time taken in seconds, which is 259147.451 seconds in this case.  $I_{leakage}$  has been calculated approximately as 11.576  $\mu A$ . Subsequently,  $R_{dcl}$  is calculated as 259147.451  $\Omega$  using (13).

$$R_{dcl} = \frac{\Delta V}{I_{leakage}} \quad (13)$$

The total average current that the sensor node with the voltage regulator extracts from the supercapacitor is 612.556  $\mu A$ , including  $I_{leakage}$ . Further,  $P_{cons}$  is measured as 1.98 mW. In contrast, the average charging current of the supercapacitor during heavy rain and empty road condition has been measured as 1.31 mA, and the average harvested power is 3.4 mW during the particular condition. Thus, it can be noted that the device harvests much more power and current compared to the consumption at any point of time, considering self-discharge process of the supercapacitor. This can ensure the self-sustainability feature of

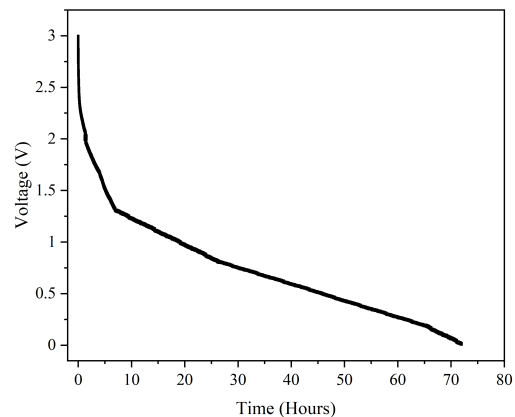


Fig. 18. Self-discharge of the supercapacitor during rainy weather

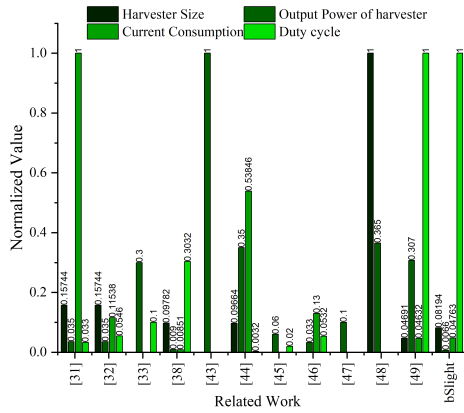


Fig. 19. Graphical representation of comparison with the state-of-the-art solar energy or artificial light energy powered LoRaWAN based devices

bSlight during heavy rain and empty road, avoiding power failure condition. Fig. 19 shows a graphical representation of comparison of the proposed work with various solar energy or artificial light energy powered LoRaWAN based energy autonomous devices with respect to four parameters such as size of harvester i.e. cross sectional area in  $mm^2$ , output power of harvester in watts, current consumption in mA and duty cycle of operation. The values have been normalized for a comprehensive understanding.

6.6 Range Testing of LoRaWAN

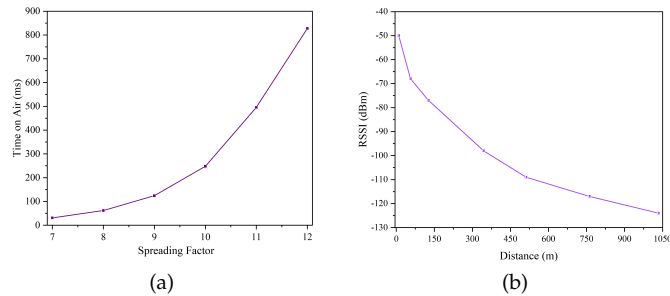


Fig. 20. (a) Calculated ToA between bSlight and LoRaWAN gateway node (b) Measured RSSI of received signal at LoRaWAN gateway node

The communication range of bSlight depends upon several factors, such as signal bandwidth, Spreading Factor (SF), coding rate, signal strength, packet loss, delay, etc. The size of data to be transferred has been kept as minimum as possible to lower power consumption as well as delay. In this work, the maximum size of data that need to be transmitted is 5 byte. Signal bandwidth and coding rate are fixed at 125 kHz and 4/5, respectively. Upon transmission of the data from bSlight, a certain amount of time it takes to reach the gateway is called as Time on Air (ToA). Further, the spreading factor has significant impact on ToA [32]. Thereby, SF has been calculated with respect to ToA using an online calculator, and the result is shown in Fig. 20(a). In order to ensure higher QoS, ToA must be lower, and it is observed to be minimum, i.e. 30.98 ms for SF 7. Thus, SF has been fixed at 7 for bSlight. The communication distance is measured when the gateway node is placed above 25

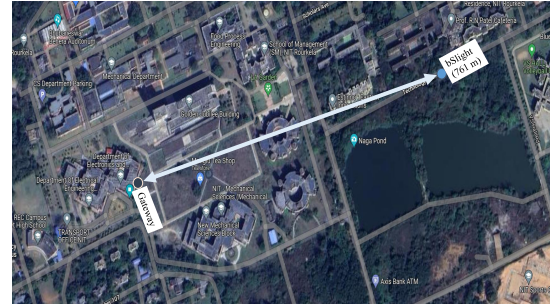


Fig. 21. Range testing of bSlight in outdoor environment

feet, and bSlight is 7 feet above ground level. Received Signal Strength Indicator (RSSI) of the transmitted signal from bSlight has been measured and shown in Fig. 20(b). It can be observed that an increase in communication distance leads to poor RSSI. The highest communication range has been measured as 1034 meters; however, Packet Delivery Rate (PDR) falls below 90% at this distance. Fig. 21 shows that the communication distance of 761 meter. PDR ranges from 90% to 100% at this distance. It falls below 90% when the distance is more than 761 meter which leads to poor QoS. Therefore, as a design consideration, the maximum communication distance is reported as 761 meter in order to ensure higher QoS of bSlight.

6.7 Performance Evaluation

There are few factors that have significant role in QoS of an energy autonomous device. Bandwidth of bSlight has been kept minimum i.e. 125 kHz, in order to ensure low power consumption. However, as per the size of data to be transferred and communication interval, the device performs well at this bandwidth. Communication delay has to be low for better QoS. ToA of the transmitted data is calculated as 30.98 ms for bSlight. The data has to be transmitted every 900 seconds in this work, implying that the calculated ToA is negligible compared to the interval. Thus, delay is reasonable in bSlight, ensuring high QoS. Power consumption is optimized to 2.022 mW which is observed to be minimal compared to state-of-the-art street light management systems. PDR varies due to communication distance; however, it is ensured to be above 90% for the tested communication range. The lifetime of bSlight depends on many factors but majorly on its storage unit. Although the exact calculation of the lifetime of a supercapacitor is challenging; however, it has a charge cycle of more than half a million. The number of

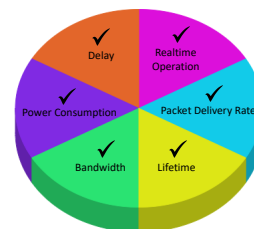


Fig. 22. QoS summary of bSlight

TABLE 4  
Comparison with State-of-the-art LoRaWAN based Solar Energy or Artificial Light Energy Powered Energy Autonomous Devices

References	Energy Source	Size of Harvester (mm)	Harvester Output	Storage	Application	Power Consumption	Current Consumption	Duty Cycle (%)
Wu <i>et al.</i> , 2018 [38]	Sunlight & Artificial light	Radius = 30	90 mW	Supercapacitor	Environmental parameter monitoring	—	75.57 $\mu$ A – 1.38 mA	15.16
Zhang <i>et al.</i> , 2019 [43]	Sunlight	—	10 W	Battery	Soil health monitoring	—	—	—
Sadowski <i>et al.</i> , 2020 [48]	Sunlight	170 x 170	3.65 W	Battery	Soil health monitoring	29.33 mW	—	—
Bhusal <i>et al.</i> , 2020 [44]	Sunlight & Artificial light	210 x 113	3.5 W	Battery	Air quality monitoring	25.9 mW	7 mA	0.16
Ali <i>et al.</i> , 2021 [33]	Sunlight	—	3 W	Battery	Air pollution monitoring	$\approx$ 14.306 mW – 14.97 mW	—	$\approx$ 5 – 6
Ramson <i>et al.</i> , 2021 [31]	Sunlight	70 x 65	350 mW	Battery	Soil health monitoring	—	13 mA	1.65
Kombo <i>et al.</i> , 2021 [45]	Sunlight	—	6 W	Battery	Under groundwater monitoring	104.081 mW	—	< 1
Petrariu <i>et al.</i> , 2021 [46]	Sunlight	—	330 mW	Battery and Supercapacitor	Environmental parameter monitoring and Geolocation tracking	—	1.69 mA	2.66
Yuksel <i>et al.</i> , 2021 [47]	Sunlight	—	1 W	Supercapacitor	Environmental parameter monitoring	380 mW	—	—
Ramson <i>et al.</i> , 2022 [32]	Sunlight	70 x 65	350 mW	Battery	Smart trashbin	—	1.5 mA	2.73
Mohanty <i>et al.</i> , 2022 [49]	Sunlight	45 x 30	307 mW	Battery	Street light management	2.012 mW	602.19 $\mu$ A	50
Current Paper (bSlight)	Sunlight & Artificial light	64 x 37	66 mW	Supercapacitor	street light management	2.022 mW	619.14 $\mu$ A	50

— represents that neither the direct data nor it relevant data from which it can be calculated is available in the original manuscript.

charge cycles utilized in a day is calculated as 60.65, considering that the average power consumption is 2.022 mW. The supercapacitor has a total of 500000 full charge cycles as per the manufacturer if charged in standard conditions. Thus, the lifetime can be calculated as 29.81 years following simple charge cycle calculation. However, it is almost impossible to ensure that the supercapacitor is getting charged on the field at standard conditions as per the manufacturer. Thereby, the lifetime can be roughly taken as 50% of the calculated value, which is more than 14.5 years. It can be noted that the other components of the device may not have this much life when deployed on the field. The life of off-the-shelf sensors and microcontrollers generally ranges between 5 to 10 years. Therefore, the overall lifetime of bSlight can be taken as 5 to 10 years. Further, bSlight follows the deadlines of the tasks as per the design algorithm which can be observed through Fig. 14. This ensures the real-time operation of bSlight. As a result, the design of bSlight takes into account and satisfies those criteria which contribute to its QoS. The summary of QoS is comprehensively presented in Fig. 22.

In order to observe the improvement done compared to existing energy autonomous devices, a comparison has been shown in Table 4. All the presented works in the table are powered from solar energy and incorporated with LoRaWAN for communication of data. The improvements compared to the existing energy autonomous devices have been written below.

- The percentage of duty cycle of the operation is 50% which is much higher compared to the existing works. This has been achieved by optimizing the power consumption of the device and critically choosing a primary task as well as secondary task according to their priority as per the demand of the application.
- In order to maintain higher percentage of duty cycle, higher size solar cells are generally preferred [8], [9]. However, in the proposed work, the device is powered using a smaller size solar cell having cross sectional area of 2355.2  $mm^2$  which is minimum compared to the existing works.
- Energy harvesting from sunlight as well as artificial light has been enabled in both [38] and bSlight to incorporate supercapacitor; however, solar cell of smaller cross sectional area has been used in the proposed

work, which provides opportunity to restrict the form factor of a device while packaging.

## 7 CONCLUSION

A supercapacitor based energy autonomous street light management system has been presented in this manuscript. It continuously detects motion around the road and adjusts the illuminance of street lights according to vehicle and pedestrian movement. It also communicates the operational status of the street light to ThingSpeak cloud using LoRaWAN gateway in every 15 minutes. This can assist the responsible authority in keeping track of the operational state of the street light so that immediate action can be urged in the event of a problem. The system incorporates low power management circuit and sensors to ensure low power consumption. It works with 50% duty cycle consuming an average current of 619.14  $\mu$ A and average power of 2.022 mW. The system is designed to harvest energy both from sunlight and artificial light using a tiny solar cell of dimension 64 mm x 37 mm x 0.22 mm and maximum output power of 66 mW to run the sensor node hence overcoming the issue of energy unavailability. The communication range has been measured as 761 m in real-word testbed. The system has been deployed in field in order to validate its feasibility.

A battery health monitoring technique for sustainable IoT devices has been proposed in [16]. Similar mechanism can be developed in future for IoT devices with supercapacitor and implemented in the proposed work in order to ensure sustainability. Security concerns can also be solved by implementing hardware mechanism in future [50].

## REFERENCES

- [1] U. Nations, "2018 revision of world urbanization prospects," May 16, 2018. [Online]. Available: <https://www.un.org/development/desa/publications/2018-revision-of-world-urbanization-prospects.html>.
- [2] S. P. Mohanty, U. Choppali and E. Kougianos, "Everything you wanted to know about smart cities: The Internet of things is the backbone," *IEEE Consumer Electronics Magazine*, vol. 5, no. 3, pp. 60-70, July 2016, doi: 10.1109/MCE.2016.2556879.
- [3] Z. Kaleem, T. M. Yoon, and C. Lee, "Energy Efficient Outdoor Light Monitoring and Control Architecture Using Embedded System," *IEEE Embedded Syst. Lett.*, vol. 8, no. 1, pp. 18–21, Mar. 2016, doi: 10.1109/LES.2015.2494598.

- [4] L. Vailshery, "IoT and non-IoT connections worldwide 2010-2025," Accessed: Mar. 8, 2021. [Online]. Available: <https://www.statista.com/statistics/1101442/iot-number-of-connected-devices-worldwide/#statisticContainer>.
- [5] H. Elahi, K. Munir, M. Eugeni, S. Atek, and P. Gaudenzi, "Energy Harvesting towards Self-Powered IoT Devices," *Energies*, vol. 13, no. 21, pp. 5528–5558, Oct. 2020, doi: 10.3390/en13215528.
- [6] S. K. Ram, B. B. Das, K. Mahapatra, S. P. Mohanty and U. Choppali, "Energy Perspectives in IoT Driven Smart Villages and Smart Cities," *IEEE Consumer Electronics Magazine*, vol. 10, no. 3, pp. 19–28, 1 May 2021, doi: 10.1109/MCE.2020.3023293.
- [7] Y. He, X. Cheng, W. Peng, and G. L. Stuber, "A survey of energy harvesting communications: models and offline optimal policies," *IEEE Commun. Mag.*, vol. 53, no. 6, pp. 79–85, Jun. 2015, doi: 10.1109/MCOM.2015.7120021.
- [8] A. H. Dehwah, M. Mousa, and C. G. Claudel, "Lessons learned on solar powered wireless sensor network deployments in urban, desert environments," *Ad Hoc Networks*, vol. 28, pp. 52–67, May 2015, doi: 10.1016/j.adhoc.2015.01.013.
- [9] M. V. Ramesh, "Design, development, and deployment of a wireless sensor network for detection of landslides," *Ad Hoc Networks*, vol. 13, pp. 2–18, Feb. 2014, doi: 10.1016/j.adhoc.2012.09.002.
- [10] G. Shahzad, H. Yang, A. W. Ahmad, and C. Lee, "Energy-Efficient Intelligent Street Lighting System Using Traffic-Adaptive Control," *IEEE Sensors J.*, vol. 16, no. 13, pp. 5397–5405, Jul. 2016, doi: 10.1109/JSEN.2016.2557345.
- [11] P. T. Daely, H. T. Reda, G. B. Satria, J. W. Kim, and S. Y. Shin, "Design of Smart LED Streetlight System for Smart City With Web-Based Management System," *IEEE Sensors J.*, vol. 17, no. 18, pp. 6100–6110, Sep. 2017, doi: 10.1109/JSEN.2017.2734101.
- [12] D. Saha, S. M. Sorif, and P. Dutta, "Weather Adaptive Intelligent Street Lighting System With Automatic Fault Management Using Boltuino Platform," in *Proc. International Conference on ICT for Smart Society (ICISS)*, 2021, pp. 1–6, doi: 10.1109/ICISS53185.2021.9533234.
- [13] A. Abdullah, S. H. Yusoff, S. A. Zaini, N. S. Midi, and S. Y. Mohamad, "Smart Street Light Using Intensity Controller," in *Proc. 7th International Conference on Computer and Communication Engineering (ICCCCE)*, Sep. 2018, pp. 1–5, doi: 10.1109/ICCCCE.2018.8539321.
- [14] S. M. Sorif, D. Saha, and P. Dutta, "Smart Street Light Management System with Automatic Brightness Adjustment Using Bolt IoT Platform," in *Proc. IEEE International IOT, Electronics and Mechatronics Conference (IEMTRONICS)*, Apr. 2021, pp. 1–6, doi: 10.1109/IEMTRONICS52119.2021.9422668.
- [15] F. Sanchez-Sutil and A. Cano-Ortega, "Smart regulation and efficiency energy system for street lighting with LoRa LPWAN," *Sustainable Cities and Society*, vol. 70, pp. 102912–102927, Jul. 2021, doi: 10.1016/j.scs.2021.102912.
- [16] A. Sinha, D. Das, V. Udutalappally and S. P. Mohanty, "iThing: Designing Next-Generation Things With Battery Health Self-Monitoring Capabilities for Sustainable IIoT," *IEEE Transactions on Instrumentation and Measurement*, vol. 71, pp. 1–9, 2022, Art no. 3528409, doi: 10.1109/TIM.2022.3216594.
- [17] Y. Jiang, Y. Shuai, X. He, X. Wen, and L. Lou, "An Energy-Efficient Street Lighting Approach Based on Traffic Parameters Measured by Wireless Sensing Technology," *IEEE Sensors J.*, vol. 21, no. 17, pp. 19134–19143, Sep. 2021, doi: 10.1109/JSEN.2021.3089208.
- [18] S. Chen, G. Xiong, J. Xu, S. Han, F.-Y. Wang, and K. Wang, "The Smart Street Lighting System Based on NB-IoT," in *Proc. Chinese Automation Congress (CAC)*, Nov. 2018, pp. 1196–1200, doi: 10.1109/CAC.2018.8623281.
- [19] F. Bellido-Outeiriño, F. Quiles-Latorre, C. Moreno-Moreno, J. Flores-Arias, I. Moreno-García, and M. Ortiz-López, "Streetlight Control System Based on Wireless Communication over DALI Protocol," *Sensors*, vol. 16, no. 5, pp. 597–619, Apr. 2016, doi: 10.3390/s16050597.
- [20] F. Leccese, "Remote-Control System of High Efficiency and Intelligent Street Lighting Using a ZigBee Network of Devices and Sensors," *IEEE Trans. Power Delivery*, vol. 28, no. 1, pp. 21–28, Jan. 2013, doi: 10.1109/TPWRD.2012.2212215.
- [21] F. Leccese, M. Cagnetti, and D. Trinca, "A Smart City Application: A Fully Controlled Street Lighting Isle Based on Raspberry-Pi Card, a ZigBee Sensor Network and WiMAX," *Sensors*, vol. 14, no. 12, pp. 24408–24424, Dec. 2014, doi: 10.3390/s141224408.
- [22] L. Yongsheng, L. Peijie, and C. Shuying, "Remote Monitoring and Control System of Solar Street Lamps Based on ZigBee Wireless Sensor Network and GPRS," in *Proc. Electronics and signal processing*, 2011, pp. 959–967.
- [23] S. K. Ram, S. R. Sahoo, B. B. Das, K. Mahapatra and S. P. Mohanty, "Eternal-Thing: A Secure Aging-Aware Solar-Energy Harvester Thing for Sustainable IoT," *IEEE Transactions on Sustainable Computing*, vol. 6, no. 2, pp. 320–333, 1 April–June 2021, doi: 10.1109/TSUSC.2020.2987616.
- [24] N. Saokaew, N. Kitsatit, T. Yongkunawut, P. N. Ayudhya, E. Mujjalinvimut, T. Sapaklom, P. Aregarot, and J. Kunthong, "Smart Street Lamp System using LoRaWAN and Artificial Intelligence PART I," in *Proc. 9th International Electrical Engineering Congress (iEECON)*, Mar. 2021, pp. 189–192, doi: 10.1109/iEECON51072.2021.9440337.
- [25] R. Kodali, and S. Yerroju, "Energy efficient smart street light," in *Proc. 3rd International Conference on Applied and Theoretical Computing and Communication Technology (iCATccT)*, Tumkur, Dec. 2017, pp. 190–193, doi: 10.1109/ICATCCCT.2017.8389131.
- [26] P. Mohanty, U. C. Pati, and K. Mahapatra, "Self-Powered Intelligent Street Light Management System for Smart City," in *Proc. IEEE 18th India Council International Conference (INDICON)*, Guwahati, Dec. 2021, pp. 1–6, doi:10.1109/INDICON52576.2021.9691575.
- [27] Y. -S. Yang, S. -H. Lee, G. -S. Chen, C. -S. Yang, Y. -M. Huang and T. -W. Hou, "An Implementation of High Efficient Smart Street Light Management System for Smart City," *IEEE Access*, vol. 8, pp. 38568–38585, Feb. 2020, doi: 10.1109/ACCESS.2020.2975708.
- [28] S. Bandopadhyaya, R. Dey, and A. Suhag, "Integrated health-care monitoring solutions for soldier using the internet of things with distributed computing," *Sustainable Computing: Informatics and Systems*, vol. 26, pp. 100378–100384, Jun. 2020, doi:10.1016/j.suscom.2020.100378.
- [29] P. Kumari, R. Mishra, H. P. Gupta, T. Dutta and S. K. Das, "An Energy Efficient Smart Metering System using Edge Computing in LoRa Network," *IEEE Trans. on Sustainable Computing*, early access, Jan. 2021, doi: 10.1109/TSUSC.2021.3049705.
- [30] S. Vishnu, S. R. J. Ramson, S. Senith, T. Anagnostopoulos, A. M. Mahfouz, X. Fan, S. Srinivasan, and A. Kirubaraj, "IoT-Enabled Solid Waste Management in Smart Cities," *Smart Cities*, vol. 4, no. 3, pp. 1004–1017, Jul. 2021, doi: 10.3390/smartcities4030053.
- [31] S. R. J. Ramson, W. D. León-Salas, Z. Brecheisen, E. J. Foster, C. T. Johnston, D. G. Schulze, T. Filley, R. Rahimi, M. J. C. V. Soto, J. A. L. Bolivar, and M. P. Málaga, "A Self-Powered, Real-Time, LoRaWAN IoT-Based Soil Health Monitoring System," *IEEE Internet of Things Journal*, vol. 8, no. 11, pp. 9278–9293, Jun. 2021, doi: 10.1109/IJOT.2021.3056586.
- [32] S. R. J. Ramson, S. Vishnu, A. A. Kirubaraj, T. Anagnostopoulos and A. M. Abu-Mahfouz, "A LoRaWAN IoT-Enabled Trash Bin Level Monitoring System," *IEEE Transactions on Industrial Informatics*, vol. 18, no. 2, pp. 786–795, Feb. 2022, doi: 10.1109/TII.2021.3078556.
- [33] S. Ali, T. Glass, B. Parr, J. Potgieter and F. Alam, "Low Cost Sensor With IoT LoRaWAN Connectivity and Machine Learning-Based Calibration for Air Pollution Monitoring," *IEEE Transactions on Instrumentation and Measurement*, vol. 70, pp. 1–11, 2021, doi: 10.1109/TIM.2020.3034109.
- [34] M. Phillip, and P. Singh, "Adaptive transmit power control algorithm for dynamic LoRa nodes in water quality monitoring system," *Sustainable Computing: Informatics and Systems*, vol. 32, pp. 100613–100621, Oct. 2021, doi:10.1016/j.suscom.2021.100613.
- [35] M. Phillip, and P. Singh, "An energy efficient algorithm for sustainable monitoring of water quality in smart cities," *Sustainable Computing: Informatics and Systems*, vol. 35, pp. 100768–100777, Jun. 2022, doi:10.1016/j.suscom.2022.100768.
- [36] W. A. Jabbar, T. Subramaniam, A. E. Ong, M. I. Shu'lb, W. Wu, and M. A. Oliveira, "LoRaWAN-Based IoT System Implementation for Long-Range Outdoor Air Quality Monitoring," *Internet of Things*, vol. 19, pp. 100540–100564, May. 2022, doi:10.1016/j.iot.2022.100540.
- [37] S. Suman and S. De, "Low Complexity Dimensioning of Sustainable Solar-Enabled Systems: A Case of Base Station," *IEEE Trans. on Sustainable Computing*, vol. 5, no. 3, pp. 438–454, Jul. 2020, doi: 10.1109/TSUSC.2019.2947642.
- [38] F. Wu, J. M. Redoute, and M. R. Yuce, "WE-Safe: A Self-Powered Wearable IoT Sensor Network for Safety Applications Based on LoRa," *IEEE Access*, vol. 6, pp. 40846–40853, 2018, doi: 10.1109/ACCESS.2018.2859383.
- [39] S. Ban, J. Zhang, L. Zhang, K. Tsay, D. Song, and X. Zou, "Charging and discharging electrochemical supercapacitors in the

presence of both parallel leakage process and electrochemical decomposition of solvent," *Electrochimica Acta*, vol. 90, pp. 542-549, Feb. 2013, doi: 10.1016/j.electacta.2012.12.056.

- [40] X. Yue et al., "Development of an Indoor Photovoltaic Energy Harvesting Module for Autonomous Sensors in Building Air Quality Applications," *IEEE Internet of Things Journal*, vol. 4, no. 6, pp. 2092-2103, Dec. 2017, doi: 10.1109/JIOT.2017.2754981.
- [41] K. E. Jeon, J. She, J. Xue, S. -H. Kim and S. Park, "IuXbeacon—A Batteryless Beacon for Green IoT: Design, Modeling, and Field Tests," *IEEE Internet of Things Journal*, vol. 6, no. 3, pp. 5001-5012, Jun. 2019, doi: 10.1109/JIOT.2019.2894798.
- [42] e-peas semiconductor. *Highly efficient, regulated dual-output, ambient energy manager for up to 7-cell solar panels with optional primary battery*. Accessed: Mar. 1, 2022. [Online]. Available: <https://e-peas.com/product/aem10941/>.
- [43] X. Zhang, M. Zhang, F. Meng, Y. Qiao, S. Xu and S. Hour, "A Low-Power Wide-Area Network Information Monitoring System by Combining NB-IoT and LoRa," *IEEE Internet of Things Journal*, vol. 6, no. 1, pp. 590-598, Feb. 2019, doi: 10.1109/JIOT.2018.2847702.
- [44] H. Bhusal, P. Khatiwada, A. Jha, J. Soumya, S. Koorapati and L. R. Cenkeramaddi, "A Self-Powered Long-range Wireless IoT Device based on LoRaWAN," in *Proc. IEEE International Symposium on Smart Electronic Systems (iSES) (Formerly iNiS)*, 2020, pp. 242-245, doi: 10.1109/iSES50453.2020.00061.
- [45] O. H. Kombo, S. Kumaran and A. Bovim, "Design and Application of a Low-Cost, Low-Power, LoRa-GSM, IoT Enabled System for Monitoring of Groundwater Resources With Energy Harvesting Integration," *IEEE Access*, vol. 9, pp. 128417-128433, 2021, doi: 10.1109/ACCESS.2021.3112519.
- [46] A. I. Petrariu, A. Lavric, E. Coca and V. Popa, "Hybrid Power Management System for LoRa Communication Using Renewable Energy," *IEEE Internet of Things Journal*, vol. 8, no. 10, pp. 8423-8436, May 2021, doi: 10.1109/JIOT.2020.3046324.
- [47] M. Yuksel, and H. Fidan, "Energy-aware system design for batteryless LPWAN devices in IoT applications," *Ad Hoc Networks*, vol. 122, pp. 102625-102645, Jul. 2021, doi: 10.1016/j.adhoc.2021.102625.
- [48] S. Sadowski, and P. Spachos, "Wireless technologies for smart agricultural monitoring using internet of things devices with energy harvesting capabilities," *Computers and Electronics in Agriculture*, vol. 172, pp. 103558-103566, Mar. 2020, doi: 10.1016/j.compag.2020.105338.
- [49] P. Mohanty, U. C. Pati, K. K. Mahapatra and S. P. Mohanty "En-Slight: Energy Autonomous Street Light Management System for Smart City," submitted for publication.
- [50] S. K. Ram, S. R. Sahoo, B. B. Das, K. K. Mahapatra, and S. P. Mohanty, "Eternal-Thing 2.0: Analog-Trojan Resilient Ripple-Less Solar Harvesting System for Sustainable IoT," *ACM Journal on Emerging Technologies in Computing Systems (JETC)*, vol. 19, no. 2, pp. 1-25, Mar. 2023, doi: 10.1145/3575800.



**Prajnyajit Mohanty** (Graduate Student Member, IEEE) received B.Tech degree in Electronics and Instrumentation Engineering from National Institute of Science and Technology, Berhampur, in 2017, and M.Tech degree in Control and Instrumentation Engineering from Veer Surendra Sai University of Technology, Burla, in 2019. He is currently pursuing Ph. D. in Electronics and Communication Engineering from National Institute of Technology Rourkela. His research interests include Energy Harvesting Systems,

Internet of Things, Low Power Embedded System Design, and Machine Learning.



**Umesh C. Pati** (Senior Member, IEEE) is a full Professor at the Department of Electronics and Communication Engineering, National Institute of Technology (NIT), Rourkela. He has obtained his B.Tech. degree in Electrical Engineering from National Institute of Technology (NIT), Rourkela, Odisha. He received both M.Tech. and Ph.D. degrees in Electrical Engineering with specialization in Instrumentation and Image Processing respectively from Indian Institute of Technology (IIT), Kharagpur. His current areas of interest are Image/Video Processing, Computer Vision, Artificial Intelligence, Internet of Things (IoT), Industrial Automation, and Instrumentation Systems. He has authored/edited two books, published over 100 articles in the peer-reviewed international journals as well as conference proceedings and filed 2 Indian patents. He has served as reviewer in a wide range of reputed international journals and conferences. He has also guest-edited special issues of Cognitive Neurodynamics and International Journal of Signal and Imaging System Engineering.



**Kamalakanta Mahapatra** (Senior Member, IEEE) Dr. Kamalakanta Mahapatra is a Professor (HAG) in Electronics and Communication Engineering Department of National Institute of Technology, Rourkela. He assumed professor position since February 2004. He obtained his B. Tech degree with Honours from Regional Engineering College, Calicut in 1985, Master's from Regional Engineering College, Rourkela in 1989 and Ph. D. from IIT Kanpur in 2000. He is a senior member of the IEEE and a fellow of the institution of Engineers (India) in ECE Division. Presently, he is the Chairman of IEEE Rourkela Sub-section and mentor of IEEE CTSoc chapter of Kolkata section. He has published several research papers in National and International Journals. He received coveted J. C. Bose award for best engineering oriented research in the year 2014. His research interests include Embedded Computing Systems, VLSI Design, Hardware Security and Industrial/Consumer/Power Electronics. He has supervised 24 PhD dissertations and 92 Master's theses.



**Saraju P. Mohanty** (Senior Member, IEEE) received the bachelor's degree (Honors) in electrical engineering from the Orissa University of Agriculture and Technology, Bhubaneswar, in 1995, the master's degree in Systems Science and Automation from the Indian Institute of Science, Bengaluru, in 1999, and the Ph.D. degree in Computer Science and Engineering from the University of South Florida, Tampa, in 2003. He is a Professor with the University of North Texas. His research is in "Smart Electronic Systems"

which has been funded by National Science Foundations (NSF), Semiconductor Research Corporation (SRC), U.S. Air Force, IUSSTF, and Mission Innovation. He has authored 450 research articles, 5 books, and invented 9 granted/pending patents. His Google Scholar h-index is 51 and i10-index is 220 with 11,000 citations. He is a recipient of 14 best paper awards, Fulbright Specialist Award in 2020, IEEE Consumer Electronics Society Outstanding Service Award in 2020, the IEEE-CS-TCVLSI Distinguished Leadership Award in 2018, and the PROSE Award for Best Textbook in Physical Sciences and Mathematics category in 2016. He has delivered 18 keynotes and served on 14 panels at various International Conferences. He has been the Editor-in-Chief of the IEEE Consumer Electronics Magazine during 2016-2021 and currently serves on the editorial board of 8 journals/transactions.